CHAPTER 4: CONCEPTUAL DESIGN

4.1. INTRODUCTION

This chapter focuses on the interface between the biological muscle system and the sEMG acquisition system. The aim is to derive a muscle model in order to incorporate the developed sensor with a control system to verify that the sensing platform is functional.

The chapter contents have a strong systems engineering (SE) backbone. The chapter starts with the functional analysis to turn the needs into a functional block diagram. The system architecture is derived from the functional block diagram to be used as a conceptual design [6]. The first step in a functional analysis is to summarise the requirements as done in the list below.

4.2. REQUIREMENTS

The primary goal is to create an HMI that sense sEMG signals. Future studies will use this sensing platform to implement proportional powered prosthetic control in Matlab®/Simulink®. Although variability is an issue, the sEMG sensor should be able to cope with variability among people.

Users should have the minimum skill and knowledge to be able to make use of the sEMG platform, which implies a user-friendly design should include easy installation and operation. Current existing systems are expensive and beyond what most patients could afford. By lowering the cost of a system, the technology could be reachable for more patients.

4.3. THE COST OF THE SYSTEM

Costing is not part of the functional analysis, and is dealt with very briefly. Current sEMG systems on the market cost around 100 000 ZAR, and a complete myoelectric prosthesis hand costs around 400 000 ZAR [59]. This is beyond the budget of the project and the budget of the intended use. The long term goal of the prosthesis hand research is to improve the affordability of powered prosthetics technology. The goal of this study is to lower the cost of sEMG technology.

Whether the marketed products will be able to perform the required functions or not, is disputable. Developing a hardware platform allows control over the functionality and quality of the final product. In figure 39 the cost versus functionality for both the buy and in-house development options are demonstrated.

The ΔY in the figure illustrates the lowered cost of the in-house development compare to the buy option. The goal is to lower the cost to below 1000 ZAR for the sEMG sensing platform. The ΔX in the figure shows the increase in functionality from “buy option” having only sEMG capabilities up to the “in-house development” having bi-directional communication with the Matlab®/Simulink® environment. This functionality allows the platform to provide output functionality to a future prosthetic control study, such as a PDM servo.

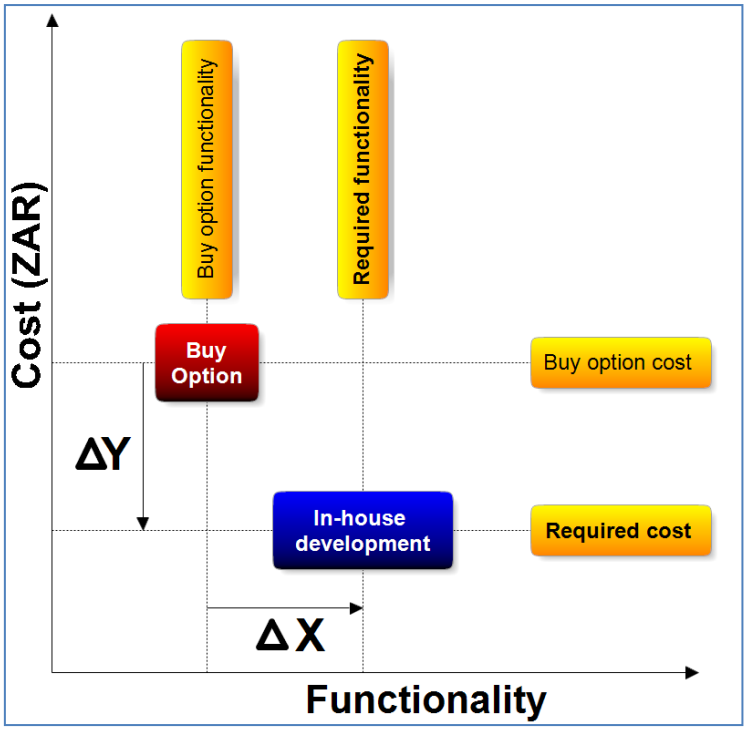

Figure 39: Cost versus functionality graph

4.4. FUNCTIONAL ANALYSIS

A functional analysis is the process of system abstraction, as it is essential to determine the correct functional needs, and design according to these needs. The first step in a functional analysis is to combine related functions into subsystem blocks that will perform similar functions [18]. The functional block diagram is shown in figure 40. Note that the top half of the diagram shows the analogue circuit functions and the bottom half shows the digital circuit functions.

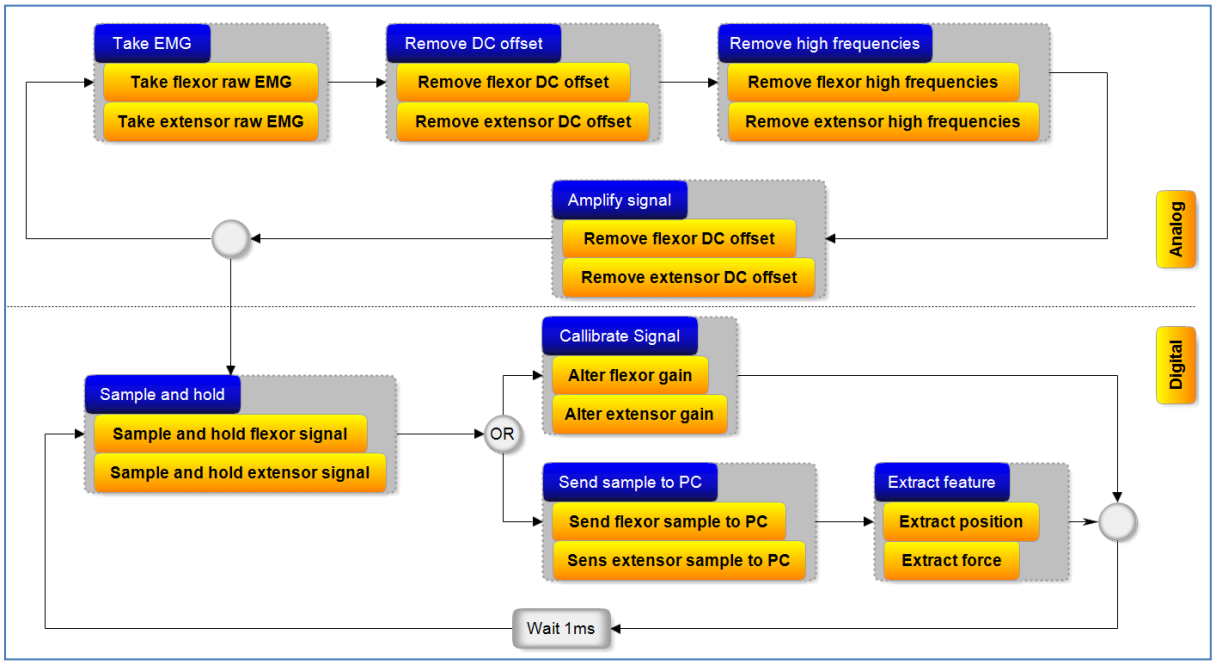

Figure 40: Functional block diagram of sEMG hardware platform

4.5. SYSTEM ARCHITECTURE

The system architecture is given in figure 41. The sEMG measuring system is divided into three components. The hardware is divided into analog electronics, digital electronics, analog power and digital power sections. The digital power is supplied by the USB port. The analog power is derived from the digital power supply with the necessary EMI suppression beads to prevent digital noise from the USB to contaminate the analog front-end. Figure 41 shows all the hardware components, except the automatic gain control, which is part of firmware. The hardware is described in the next chapter.
The USB stack and drivers from Microchip® are used as firmware interface with a PC, the push buttons, LEDs, automatic gain control interface and calibration algorithm are programmed in the firmware. The Software implementation is done in Matlab®/Simulink®. The implementation consists of a sEMG decoding algorithm to extract the position and force of the recorded antagonist muscles.

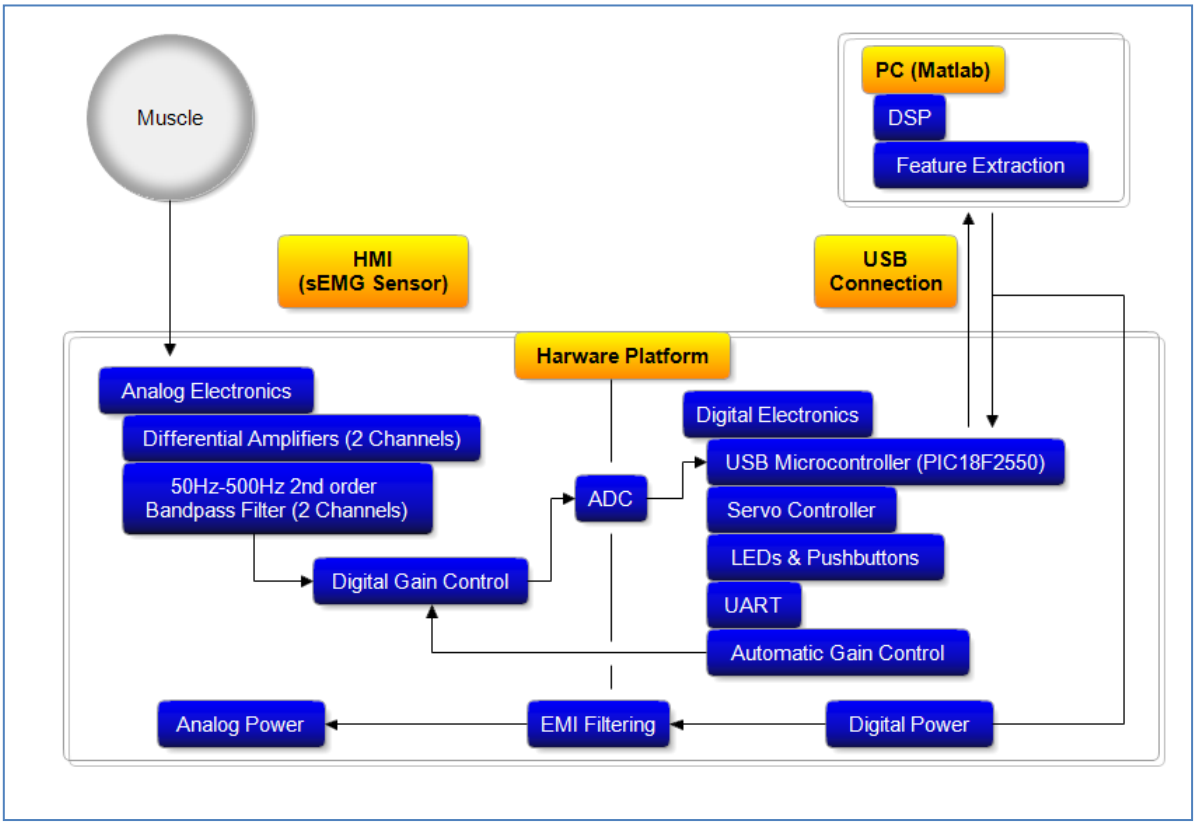

Figure 41: System architecture of sEMG hardware platform

4.6. SEMG DECODING ALGORITHM

All digital signal processing (DSP) algorithms regarding this study are implemented in Matlab®/Simulink®. The normalisation process involves the scaling of the sensor range, and the extraction of muscle activity. Pattern libraries may be trendy, but mismatches that occur in the decoding process may be frustrating. A proposed algorithm to extract reliable information from the differential sEMG signals. The extracted information can be used in future for proportional control.

4.6.1. MUSCLE ACTIVITY AND VISUAL FEEDBACK

The natural feedback system of the PNS gives an indication of muscle effort and position, allowing a person to perform tasks without viewing what his/her limbs are doing. However, when a precise muscle action is desired, visual feedback is required. This suggests that the PNS is not precise in muscle position and force calculation.

4.6.2. ANTAGONIST MUSCLE MODEL

Hill's muscle model uses different symbol convention for the muscle elements than the electrical symbol convention. The Hill symbol convention will be used throughout the study, although the electrical equivalent circuit for the antagonist muscle model is illustrated in figures that follow.

The use of Hill's muscle model requires the assumption that the muscle model is linear for concentric muscle contractions. The error that may appear due to this approximation could be eliminated by the intuitive human brain function with the aid of visual feedback. Elastic element spring constants and other transfer function constants' values cannot be determined. This is due to the difficulty in the measuring thereof, as well as the variability of these constants from person to person. The purpose of this muscle derivation is to create an understanding of proportional control and to show the relationship between the different domains and their interfaces.

Any joint in the human body has two sets of antagonous (flexor and extensor) muscles since a muscle can only perform work as it contracts. The antagonist muscles are modeled by a pulley system as shown in figure 42. The line and pulley that connects the two muscle models represents the tendons that connect the muscles to the phalanges. Two of Hill's muscle models are added to the pulley system to represent the antagonist muscles. Figure 43 is the diagram that will be used in the antagonist muscle model, showing the crucial parts taken from figure 42.

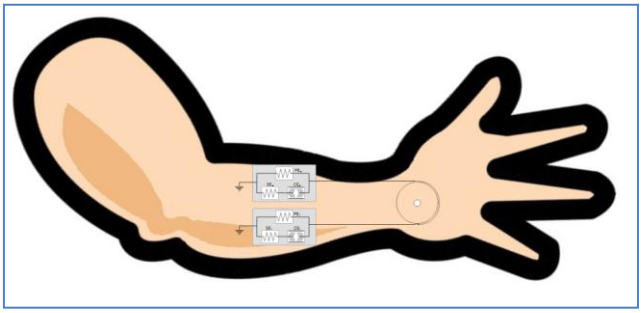

Figure 42: Pulley system of antagonist muscles' joints in hand

The ground symbol in the figure refers to the muscle's side that is fixed to a rigid part of the person's skeleton. The agonist extensor muscle is the top muscle that extends the finger, the bottom antagonist (opposing) muscle flexes the finger.

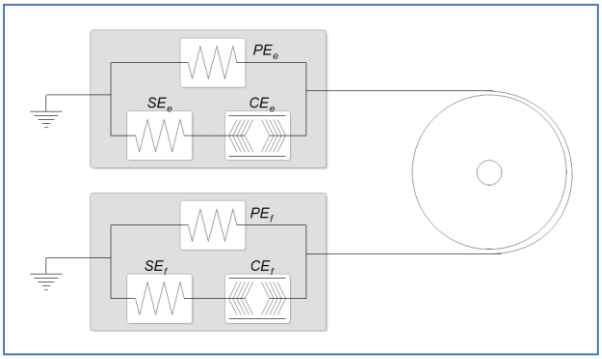

Figure 43: Antagonist muscle model diagram

To differentiate between the muscle-elements from the two muscles, subscripts are added. All the muscle elements from the extensor muscle are written with a subscript *e* and the flexor muscle's elements are written with a subscript *f*. For example, the name of the contractile-element inside the extensor muscle is called CE_f , and the force generated by this element is $Force_{CEf.}$

Concerning all antagonist muscle model examples, it is assumed that concentric muscle contractions occur and the finger is allowed to contract or relax without any load. Another assumption made, is that the pulley mechanism of the joint is considered frictionless, as it is well known that the normal human's joints are well lubricated. To demonstrate the antagonist muscle model's functionality refer to figure 44 for the following paragraph.

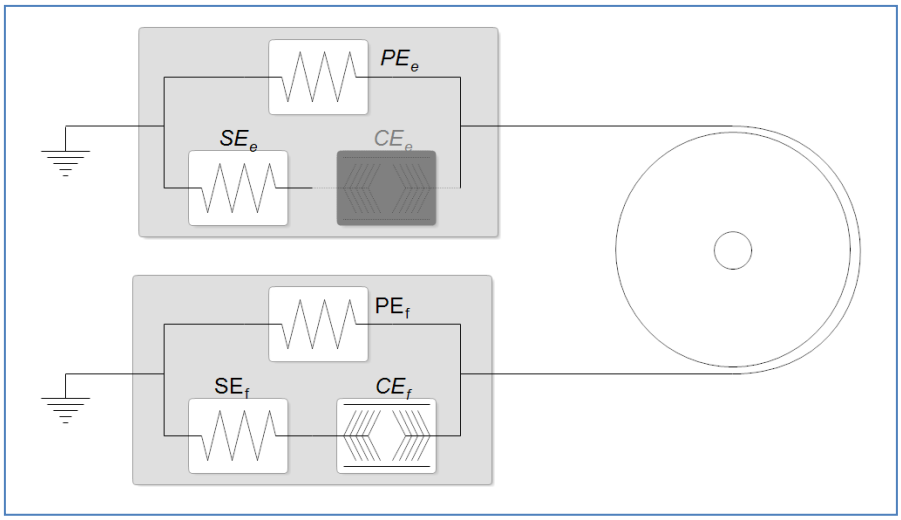

Figure 44: Antagonist muscle model simplified for flexor muscle

When the flexor muscle contracts, the extensor muscle relaxes. CE_e is omitted (indicated by darkening elements), leaving the following elements and the equation for the effort CE_f being sensed by sEMG electrodes across the flexor muscle. The across-variable force generated by the CE_f is calculated using Kirchhoff's current law using the inter-muscle tendon as the node.

Figure 45 shows the electrical equivalent circuit for the mechanical antagonist muscle model.

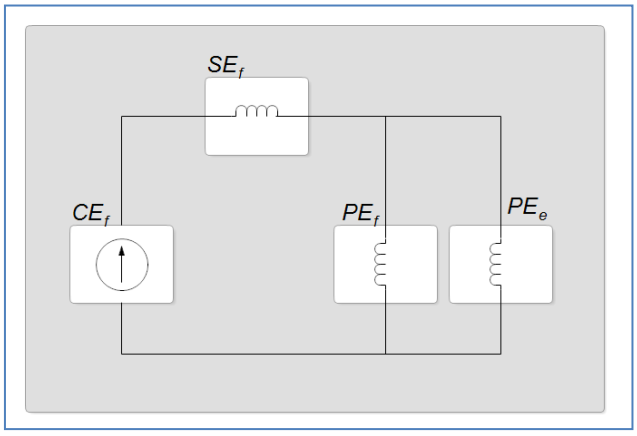

Figure 45: Equivalent electrical circuit for mechanical antagonist muscle model

The equation for the force generated by CE_f is given by

$$Force_{CE_f} = K_{SE_f} . SE_f + K_{PE_f} . \left(\frac{PE_f . K_{PE_e}}{PE_f + K_{PE_e}} \right) . PE_e \, , \qquad 4\text{-}1$$

where K_{PEf}, K_{SEf} and K_{PEe} the spring constants of the elastic elements.

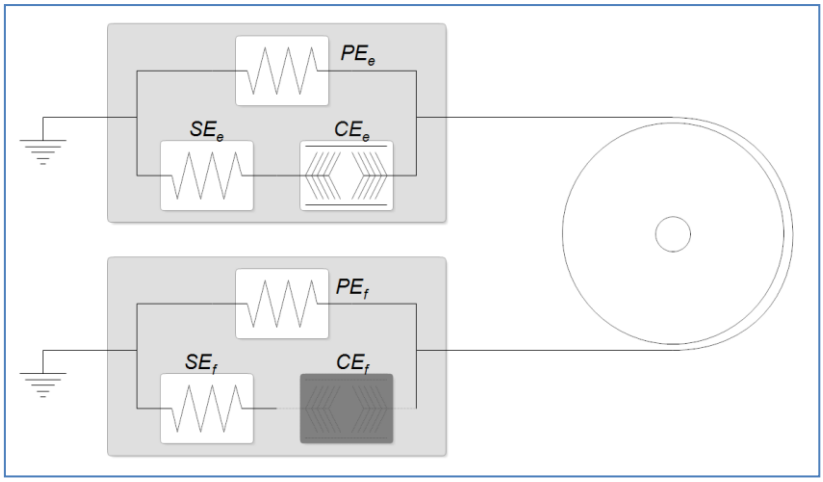

Figure 46: Antagonist muscle model simplified for extensor muscle

In figure 46, when the extensor muscle contracts, the flexor muscle relaxes. CE_f is omitted, leaving the following elements and the equation for the effort CE_e being sensed by sEMG electrodes across the flexor muscle. The across-variable force generated by the CE_e is calculated according to Kirchhoff's current law, using the inter-muscle tendon as the node. The equation for the force generated by the CE_e is given by

$$Force_{CE_e} = K_{SE_e}.SE_e + K_{PE_e}.\frac{PE_e.K_{PE_f}}{PE_e+K_{PE_f}}.PE_f\ , \qquad 4\text{-}2$$

where K_{SEf}, K_{PEe} and K_{PEf} the spring constants of the elastic elements.

4.6.3. AMPUTATED ANTAGONIST MUSCLE MODEL

The derivation of an amputated muscle model is important, since the sEMG would be used to replace the parts lost by an amputee. In the case of a wrist amputation the joints' pulley systems is changed. The pink part in figure 47 shows the pulley system removed by the amputation. When the amputation occurs, surgeons reconnect remaining muscles to the nearest rigid bone. This allow the muscle, firstly to cover the exposed bone and, secondly to give the muscle resistance to pull against and allowing the muscle to exercise and remain healthy [26].

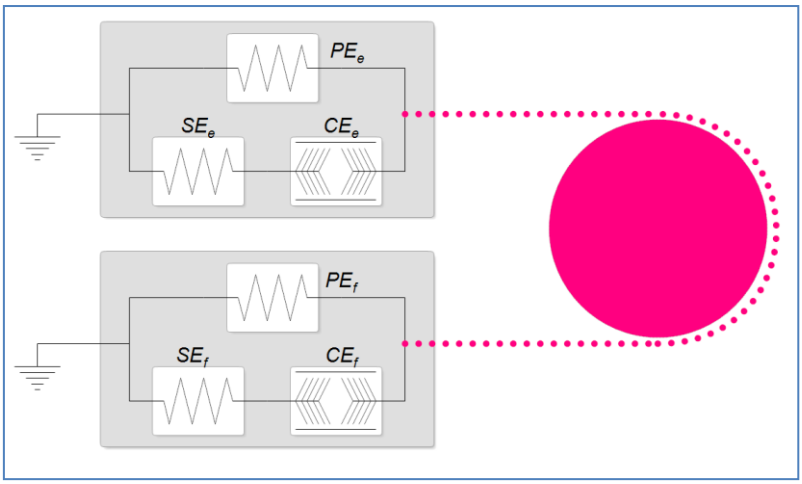

Figure 47: Pulley system removed by a wrist amputation

As the muscles are connected both ends to a rigid part of the patient's skeleton, the antagonist muscle model for an amputee differs in the sense that both ends of the muscles in the model are connected to ground as illustrated in figure 48.

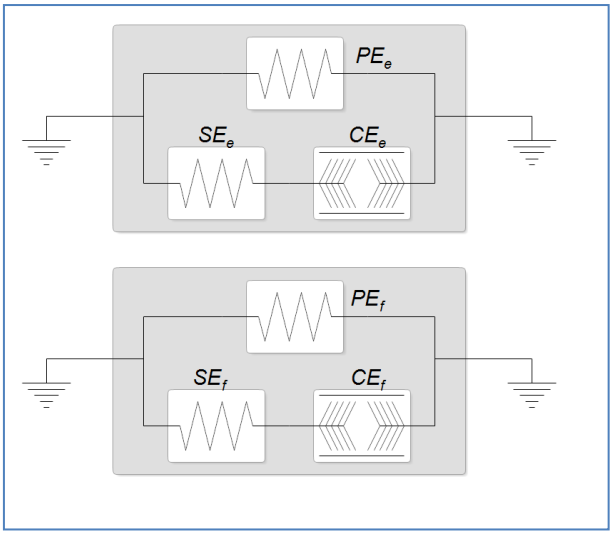

Figure 48: Amputated antagonist muscle model

For all amputated antagonist muscle model examples, it is assumed that isometric muscle contractions occur as the muscles are fixed to rigid parts of the skeleton on both ends and the muscles can't contract. To demonstrate the amputated antagonist muscle model's functionality, refer to figure 49 for the following paragraph.

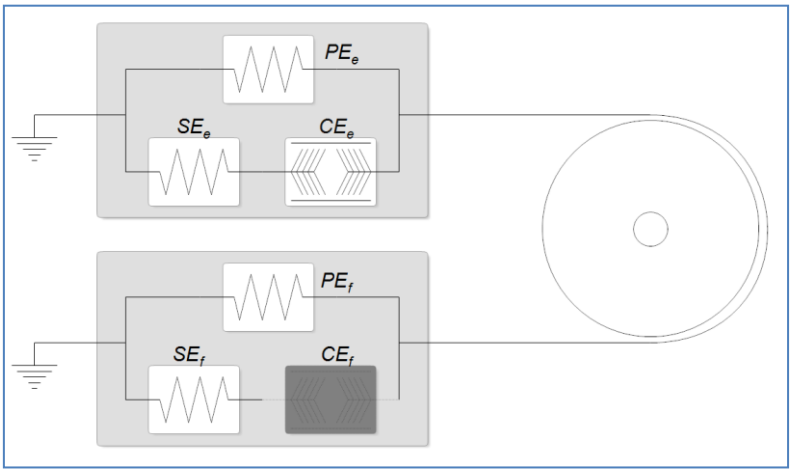

Figure 49: Amputated flexor muscle model

When the flexor muscle contracts, since the extensor muscle is no longer part of the flexor muscle's motion, and the elastic element PE_f is fixed between the grounds, the equation for the effort CE_f being sensed by sEMG electrodes across the flexor muscle are derived again using Kirchhoff's node law [47]. The electrical equivalent of the muscle model is illustrated in figure 49, with figure 50 an illustration of the elements eliminated for the amputated flexor muscle model.

The equation for the force generated by the CE_f is given by

$$Force_{CE_f} = K_{SEf}.SE_f\ , \qquad 4\text{-}3$$

where K_{SEf} is the spring constants of the elastic element SE_f.

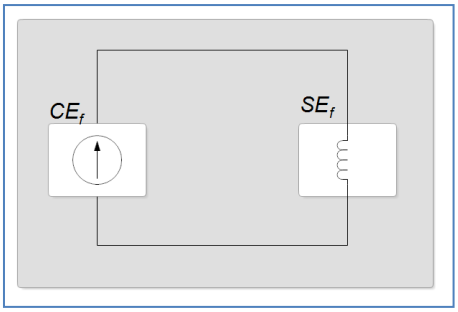

Figure 50: Simplified amputated flexor muscle model

In figure 49 when the extensor muscle contracts, since the flexor muscle is no longer part of the extensor muscle's motion, and the elastic element PE_e is fixed between the grounds the equation for the effort CE_e being sensed by sEMG electrodes across the flexor muscle are derived again using Kirchhoff's node law [47]. The equation for the force generated by the CE_e is given by

$$Force_{CE_e} = K_{SEe}.SE_e \ , \qquad 4\text{-}4$$

where K_{SEe} is the spring constants of the elastic element SE_e.

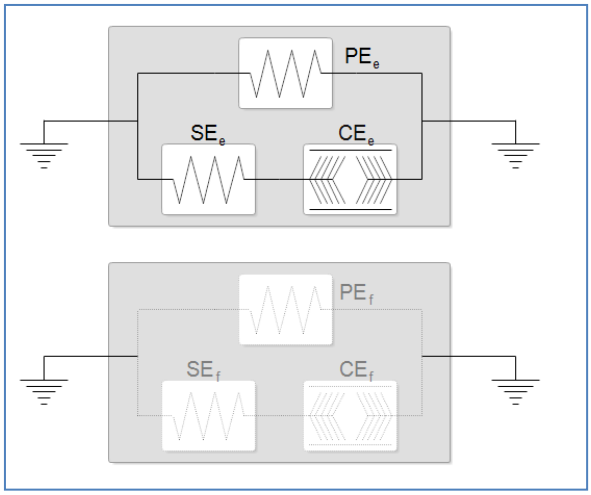

Figure 51: Amputated antagonist muscle model simplified for extensor muscle

4.6.4. PROPORTIONAL CONTROL

As discussed, some cases a linear relationship between muscle model elements is not present. Consequently, the muscle element that senses muscle position (SE or Golgi tendon organ) is non-linear. But somehow, a person is able to adapt to this non-linearity. This muscle model makes use of the assumption that the muscle model is linear for concentric muscle contractions, and the error that may appear due to this approximation could be eliminated by the intuitive human brain function with the aid of visual feedback.

The antagonist muscle model shows how the two antagonist muscles found in each degree of freedom inside the human body opposes each other's movement. From experimental results when a firm grip is held, the sEMG signals of the antagonist muscles. The net activity of the hand would of course be the sum of both muscles net activity. Any difference in the net activity of both muscles would suggest a net force in the direction of the muscle with the larger net activity. Due to the elastic elements in both muscles, the joint stretches out towards the muscle with the larger net activity's direction.

Figure 52 shows the dual channel sEMG with the muscle model. The circuit includes a sample and hold circuit to convert the analog signals into digital arrays. The signal decoding circuit diagram shown in figure 52 subtracts the antagonist muscle activities to decode the position, and the sum to decode the force (or effort). From experimental results, the signal contains noise due to the irregular firing of MUAPTs [26]. A moving average filter of 200 samples (equivalent of 200ms of samples at 1ksps) eliminates the noise, and does not have a noticeable effect on the response time of the system.

The position output will be tested for proportional accuracy, but the force result will not be tested for accuracy, but it serves as a measure of total muscle effort of both flexor and extensor muscle groups.

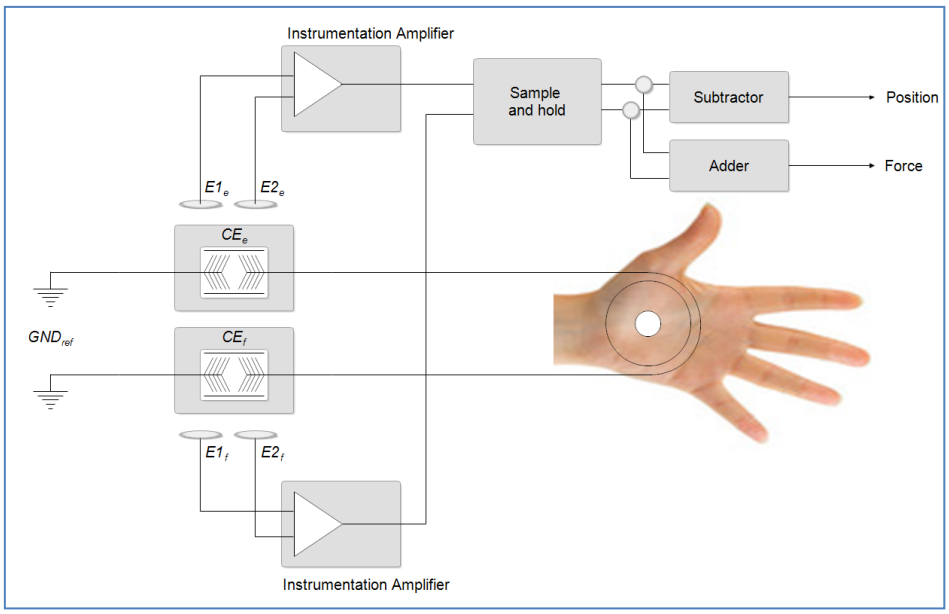

Figure 52: Antagonist muscle sEMG for proportional control algorithm

The electrodes shown in figure 52 require a transfer function to connect the *CE* from the muscle model to the sEMG amplifier's electrodes. The sum of the voltages the MUAPTs generate across the muscle tissue, are modeled as a current controlled voltage source (CCVS). Figure 53 illustrates the symbols for the CCVS. The sum of the MUAPTs equals the total *CE* effort, as the superposition principle is valid for any linear transfer function [40].

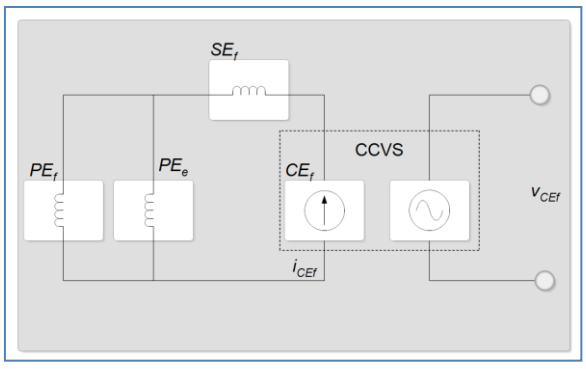

Figure 53: Transfer function of the CE

The equation for the CCVS is given by

$$VCE_f = A_{CEf}.i_{CEf} \quad , \qquad 4\text{-}5$$

where A_{CEf} is the approximated factor by which the i_{CEf} is assumed to be proportionally related to the voltage measured across the CE_f. V_{CEf} is the sEMG voltage sensed by the flexor muscle group electrode pair.

To conclude, the muscle model in its simplest form caters for both normal and amputated anatomist muscle functionality, as the derivation of each case reveals a first order DE. The algorithm is given in the next section, as it is combined with variability minimisation.

4.7. CONTROL ALGORITHM

An auto-calibration algorithm is implemented in firmware of sensors using automatic gain control to normalise the input signals for various patients. EMI filtering on USB will be added to the circuit, and EMC design guidelines for PCB layout will be followed to ensure that the SNR will be minimised. By adding an RC filter in the differential amplifier circuit design using bypass capacitors to eliminate DC gain, and allow AC gain, DC-offset errors can be minimised [48] Noise (muscle crosstalk or EMI) in the system will be common to all inputs and eliminated, because the proportional control algorithm compares the two antagonist muscles differentially. Figure 54 illustrates the importance of the signal scaling for the decoding of the sEMG signals.

The position is decoded by the subtraction of the signals, given by the equation

$$P = A - B \tag{4-5}$$

where P is the normalised position output, and A and B are the two sEMG signals sensed by the sensing platform.

The position is decoded by the subtraction of the signals, given by the equation

$$F = A + B \tag{4-6}$$

where F is the normalised force output, and A and B are the two sEMG signals sensed by the sensing platform.

Signal scaling must be done to the output before it can be compared to a position table used to control a PDM servo. The normalised signals shown in the figure is normalised by the addition of AGCs in each of the sEMG channels.

The decoding algorithm (figure 60) and calibration algorithm (figure 61) is discussed in chapter 5.

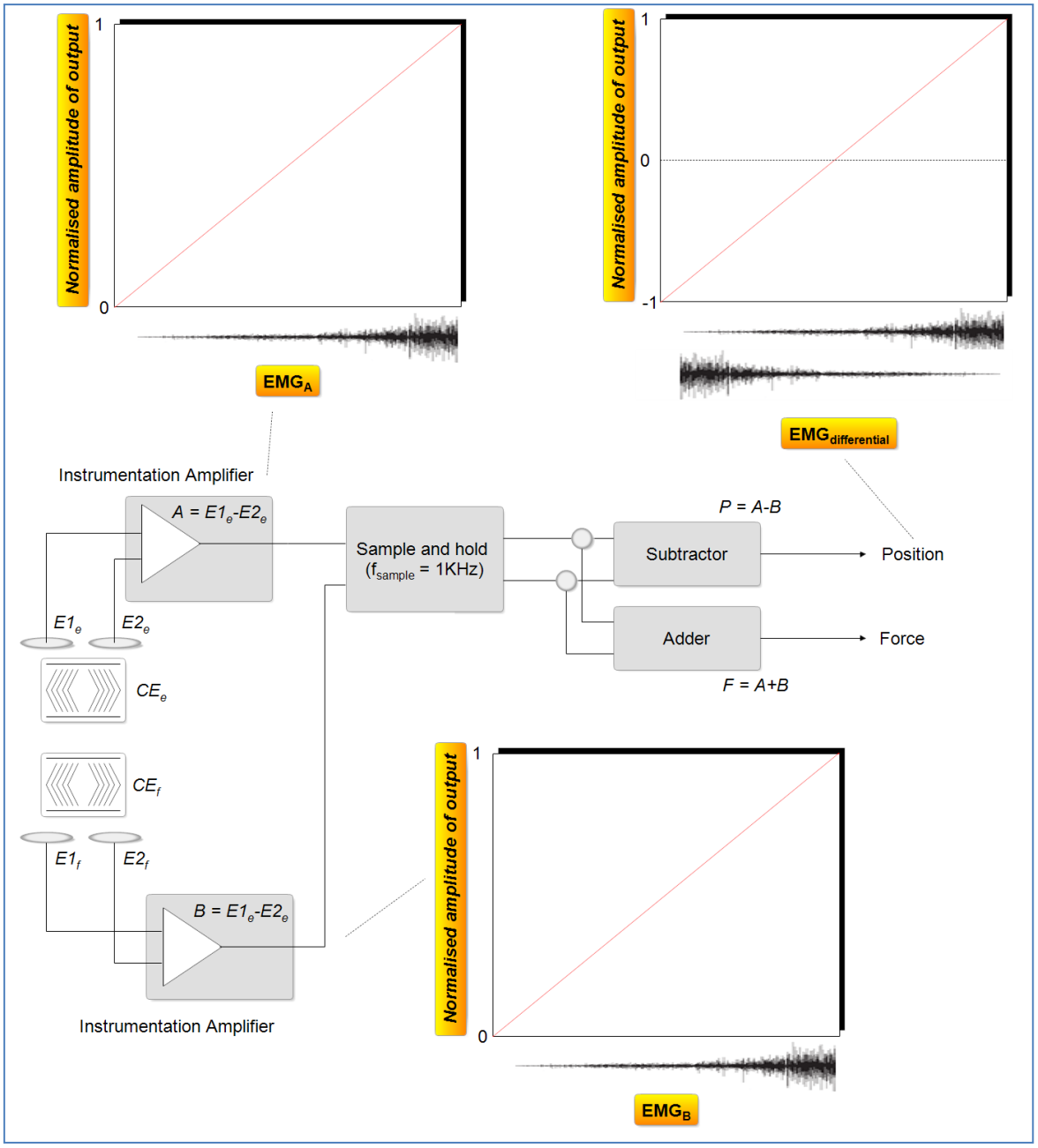

Figure 54: Decoding algorithm circuit diagram

4.8. ELECTRODE MODEL

sEMG electrodes exist for a while, and the Ag/AgCl types are believed to be superior over all of the surface electrode types [26]. As affordability forms part of the criteria, the possibility to use inexpensive substitute electrodes made from any metal such as stainless steel, may affect the performance of the EMG amplifier. This section shows how an inexpensive set of electrodes are suitable for sEMG measurement. By focusing on the input impedance of the EMG amplifier, the signal transfer function is determined.

Amplifiers usually have a DC and AC small signal model. The sEMG amplifier design is designed to amplify only AC, therefore it will be sufficient to derive only the electrode model for AC characteristics.

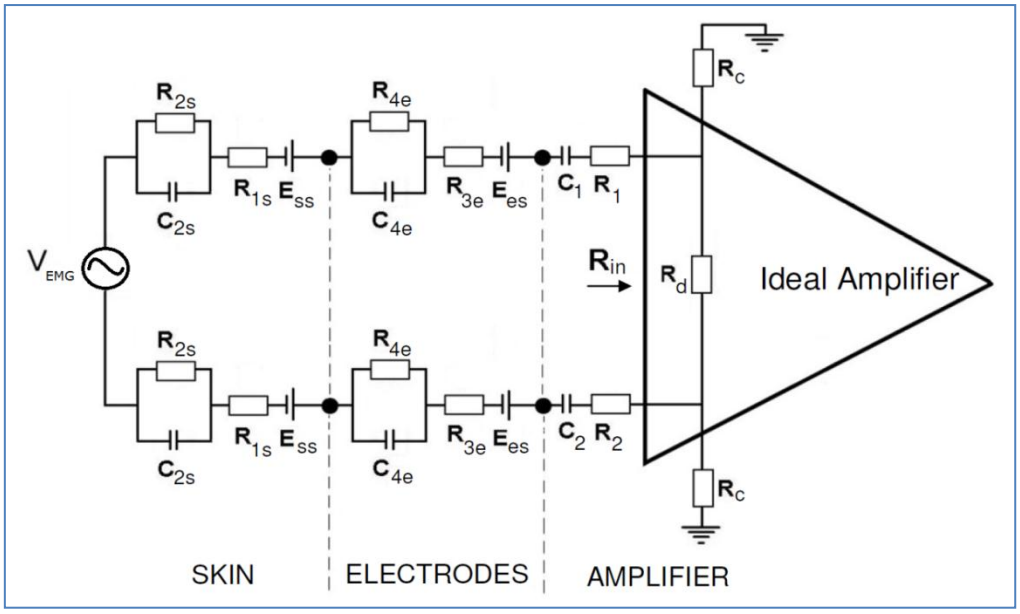

Figure 55: SEMG using identical electrodes and differential amplifier [41]

An EMG amplifier is a signal amplifier meaning that only the signal voltages will be used in the transfer functions. The efficiency of which the signal is transferred from the patient to the sEMG platform depends on the ratio between the skin-electrode impedance, and the input impedance of the instrumentation amplifier. The calculation is therefore based on a voltage divider between input impedance of the instrumentation amplifier and the electrodes.

$$\eta = \%\, efficiency = \frac{Z_{Amplifier}}{\sum Impedances\ in\ loop} .100 \qquad 4\text{-}6$$

$$\eta = \frac{Z_{Amplifier}}{Z_{E1}+Z_{E2}+Z_{Instrumentation\ Amplifier}} .100 \qquad 4\text{-}7$$

The electrode model for a sEMG system is simplified, with the assumption that the capacitance inside electrodes has no contribution to the efficiency of the system. The input impedance of a typical instrumentation amplifier is given as

$$Z_{Amplifier} = 100\ G\Omega$$

Expensive Ag/AgCl electrodes are superior and have the lowest impedance per electrode is given as

$$Z_{AgAgCl} = 5k\Omega\ [35]$$

In search of a suitable inexpensive material, if stainless steel buttons used as electrodes, their experimental impedance measured per electrode is

$$Z_{SS} = 2.5M\Omega\ (experimental\ result)$$

The efficiency of both electrodes is calculated using equation 4-7, the

$$\eta_{AgAgCl} = \frac{100\ G\Omega}{5K\Omega + 5K\Omega + 100\ G\Omega} = \ 99.99999\% \approx 100\%$$

$$\eta_{SS} = \frac{100G\Omega}{2.5M\Omega + 2.5M\Omega + 100\ G\Omega} = 99.9950002\% \approx 100\%$$

This proves that, although the Ag/AgCl electrodes have a higher efficiency, inexpensive electrodes are suitable for the use of sEMG measurements. Previous studies show that electrodes with an impedance of around *2 MΩ* exist and can be used if the input impedance of the differential amplifier is greater than *1.3 GΩ* [41]. The proposed differential amplifier has an input impedance of *100 GΩ*, and satisfies this condition.

Older research suggested the use of Ag/AgCl electrodes was crucial, but it might be because the older instrumentation amplifiers had lower input impedance and was more affected by poor conducting electrodes when the first EMG amplifiers appeared.

4.9. CONCLUSION

The main focus on this chapter is to develop the concepts for functional hardware with the focus on functionality and cost. The possibility to lower the cost is addressed by the use of inexpensive electrodes. This is shown through the efficiency of the HMI when stainless steel electrodes are used instead of Ag/AgCl electrodes.

The circuit layout caters for the possibility to use the sensing platform for future studies on proportional control. The antagonist muscle model shows what the hardware should provide in terms of signal output. The assumption made is that the muscle model's elastic elements function in a linear region.